

## Fermi Surface Nesting and Phonon Frequency Gap Drive Anomalous Thermal Transport

Chunhua Li,<sup>1</sup> Navaneetha K. Ravichandran,<sup>1</sup> Lucas Lindsay,<sup>2</sup> and David Broido<sup>1,\*</sup>

<sup>1</sup>*Department of Physics, Boston College, Chestnut Hill, Massachusetts 02467, USA*

<sup>2</sup>*Materials Science and Technology Division, Oak Ridge National Laboratory, Oak Ridge, Tennessee 37831, USA*



(Received 21 June 2018; published 22 October 2018)

The lattice thermal conductivity,  $k_L$ , of typical metallic and nonmetallic crystals decreases rapidly with increasing temperature because phonons interact more strongly with other phonons than they do with electrons. Using first principles calculations, we show that  $k_L$  can become nearly independent of temperature in metals that have nested Fermi surfaces and large frequency gaps between acoustic and optic phonons. Then, the interactions between phonons and electrons become much stronger than the mutual interactions between phonons, giving the fundamentally different  $k_L$  behavior. This striking trend is revealed here in the group V transition metal carbides, vanadium carbide, niobium carbide, and tantalum carbide, and it should also occur in several other metal compounds. This work gives insights into the physics of heat conduction in solids and identifies a new heat flow regime driven by the interplay between Fermi surfaces and phonon dispersions.

DOI: 10.1103/PhysRevLett.121.175901

In nonmagnetic electrical insulators, heat is carried by phonons. Intrinsic thermal resistance arises from mutual interactions among phonons caused by the anharmonicity of the interatomic potential [1,2]. Around and above room temperature, the lattice thermal conductivity  $k_L$  decreases sharply with temperature,  $T$  with  $k_L \sim 1/T$  above the Debye temperature of the material. In metals, heat is carried by electrons and phonons, and their mutual interactions add to the lattice thermal resistance beyond that from phonon-phonon scattering alone. Heat conduction in metals was described qualitatively by Makinson eighty years ago [3]. He showed that the contribution to thermal conduction from phonons involves a temperature dependent competition between phonon-phonon and phonon-electron interactions, with the former dominating the behavior at high  $T$  and the latter dominating at low  $T$ . Specifically,  $k_L$  limited only by phonon-electron scattering tends to zero at low  $T$  and becomes temperature independent at high  $T$ . Since  $k_L$  limited only by anharmonic phonon-phonon interactions decreases monotonically with increasing  $T$ , a temperature crossover occurs below which phonon-electron scattering dominates and above which phonon-phonon scattering dominates [2,3]. Simple estimates [2] show that this crossover should occur well below room temperature so that around and above room temperature phonon-phonon scattering should be far stronger than phonon-electron scattering. Such behavior has been confirmed in recent *ab initio* calculations of  $k_L$  for the common metals, Al, Cu, Ag, Au, Ni, Pt [4,5]. It thus appears that the strong monotonic decrease in  $k_L$  with increasing  $T$  above room temperature is a universal behavior of all nonmagnetic crystals, regardless of whether they are metallic or nonmetallic.

In this Letter, we show using a first principles theory that a strikingly different temperature dependence of  $k_L$  can occur in metallic compounds that combine nested Fermi surfaces with specific vibrational properties of the atomic lattice. Fermi surface nesting (FSN) contributes to strong electron-phonon interactions, and it has been the subject of intense interest for decades in the study of strongly correlated electron systems and phenomena such as charge density waves and superconductivity [6–8]. To our knowledge, the influence of FSN on heat conduction has not been rigorously investigated before. We demonstrate that FSN combined with particular phonon properties can yield anomalously weak phonon-phonon interactions *simultaneously* with strong phonon-electron interactions, which is opposite to the typical behavior. This interplay between the structure of the Fermi surface and the vibrational properties of the atomic lattice makes  $k_L$  nearly temperature independent around room temperature and extending well above it.

To demonstrate the effect of this novel interplay between the electronic and phononic energy spectra, we present results for two classes of transition metal carbides (TMCs). We show that the unusual temperature independence occurs in the group V TMCs, VC, NbC, and TaC, where Fermi surface nesting is known to occur. In contrast, the group IV TMCs, TiC, ZrC, and HfC, which do not have nested Fermi surfaces, show the typical behavior above room temperature,  $k_L \sim 1/T$ .

*First principles theory.*—We have implemented a first principles approach to calculate the  $k_L$  of TMCs. These materials crystallize in the rocksalt structure and are known as refractory compounds because of their extreme hardness and high melting points [9–11], which stem from strong covalent bonding [12]. Phonons are taken to scatter (i) with

other phonons—three-phonon scattering is the lowest-order intrinsic process, (ii) from isotopes—these produce a mass disorder that scatters phonons [13], and (iii) with electrons. Harmonic interatomic force constants (IFCs) are calculated using density functional perturbation theory (DFPT) [14]. From these, phonon modes, acoustic velocities and phonon-isotope scattering rates [13] are obtained. Anharmonic IFCs are calculated using a supercell approach, from which phonon-phonon scattering rates are determined [15]. Thermal expansion is incorporated within the quasiharmonic approximation. Further details are given in the Supplemental Material [16]. We note that while FSN can indicate strong electron correlations, such as occurs in TaS<sub>2</sub> and TaSe<sub>2</sub>, this does not appear to be the case for the TMCs whose properties have been accurately described by density functional theory [23,24] without including strong electron correlation corrections using, e.g., DFT + U or dynamical mean field theory.

The scattering rates of phonons with wave vector  $\mathbf{q}$  and polarization  $j$ , by electrons are [2,25–28]

$$\frac{1}{\tau_{\text{ph-el}}^L} = \frac{2\pi\Omega_0}{\hbar} \sum_{mn} \int \frac{d\mathbf{k}}{4\pi^3} |g_{nm,j}^{\text{SE}}(\mathbf{k}, \mathbf{q})|^2 [f_0(\varepsilon_{n\mathbf{k}}) - f_0(\varepsilon_{m\mathbf{k}+\mathbf{q}})] \times \delta(\varepsilon_{m\mathbf{k}+\mathbf{q}} - \varepsilon_{n\mathbf{k}} - \hbar\omega_{j\mathbf{q}}). \quad (1)$$

Here,  $\Omega_0$  is the volume of the unit cell,  $\varepsilon_{n\mathbf{k}}$  and  $\varepsilon_{m\mathbf{k}+\mathbf{q}}$  are electron energies in the initial ( $n, \mathbf{k}$ ) and the final ( $m, \mathbf{k} + \mathbf{q}$ ) states,  $\hbar\omega_{j\mathbf{q}}$  is the energy of the phonon, the sums are over the electron bands,  $n, m$ ;  $f_0$  is the Fermi distribution, and  $g_{nm,j}^{\text{SE}}(\mathbf{k}, \mathbf{q})$  is the electron-phonon scattering matrix element. IFCs, phonon frequencies, and electron energies are calculated using the QUANTUM ESPRESSO package [29,30] with norm-conserving pseudopotentials in the generalized gradient approximation. The electron-phonon matrix elements,  $g_{nm,j}^{\text{SE}}(\mathbf{k}, \mathbf{q})$ , are evaluated *ab initio* using the electron-phonon Wannier code [25–27,31]. The total phonon scattering rates are obtained from Mathiessen's rule:  $1/\tau_{\text{tot}}^L = 1/\tau_{\text{ph-ph}}^L + 1/\tau_{\text{ph-iso}}^L + 1/\tau_{\text{ph-el}}^L$ , where  $1/\tau_{\text{ph-ph}}^L$  and  $1/\tau_{\text{ph-iso}}^L$  are the three-phonon and phonon-isotope scattering rates, respectively, determined *ab initio*. For further details see Ref. [16].

The lattice thermal conductivity  $k_L$  can be expressed as

$$k_L^{\alpha\beta} = \sum_{\lambda} C_{\lambda} v_{\lambda\alpha} v_{\lambda\beta} \tau_{\lambda}^L, \quad (2)$$

where the sum is over all phonon modes  $\lambda = (j, \mathbf{q})$ ,  $C_{\lambda} = \hbar\omega_{\lambda}(\partial n_{\lambda}^0/\partial T)/V$  is the specific heat capacity per phonon mode,  $n_{\lambda}^0$  is the Bose factor at temperature  $T$ ,  $\mathbf{v}_{\lambda}$  is the velocity of mode  $\lambda$ ;  $\alpha$  and  $\beta$  are Cartesian components, and  $V$  is the crystal volume. The phonon transport lifetime in mode  $\lambda$ ,  $\tau_{\lambda}^L$ , is obtained by solving the Peierls-Boltzmann transport equation (PBE) for the nonequilibrium phonon distribution that results from a small temperature gradient

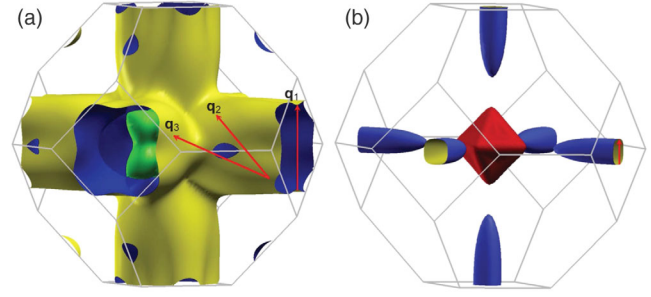


FIG. 1. Fermi surface of (a) NbC and (b) TiC calculated from first principles. Images prepared using XCRYSDEN [41]. The red arrows show the three nesting vectors with lengths 0.66 (in units of  $2\pi/a$ ) along  $\Gamma$ -X, 0.71 along  $\Gamma$ -K, and at the  $L$  point for NbC. Possible nesting vector for TiC also shown.

applied along crystallographic axis direction  $\beta$ . Solution of the PBE is accomplished using an iterative approach described previously [32–35]. The solution incorporates the quantum-mechanical scattering rates, and it goes beyond the commonly used relaxation time approximation in properly accounting for the difference between momentum-conserving normal phonon-phonon scattering processes, and resistive umklapp phonon-phonon processes [1,2]. The phonon-electron scattering is included only within the relaxation-time approximation.

*Anomalous thermal transport.*—Figure 1(a) shows the calculated Fermi surface for NbC. The six arms of this surface have roughly square cross section resulting in large parallel regions connected by specific phonon wave vectors, which defines some of the nesting. In fact, Weber [36] showed that a roughly cubic surface of nesting vectors exists in the phonon Brillouin zone. There are three nesting vectors along [100], [110], and [111] high-symmetry directions [red arrows in Fig. 1(a)]. The nesting regions give rise to strong interactions between electrons and phonons, which renormalize some phonon energies producing phonon anomalies [23,24,36–39]. Figure 2(a) shows the calculated phonon dispersions for NbC illustrating these well-known phonon anomalies [40].

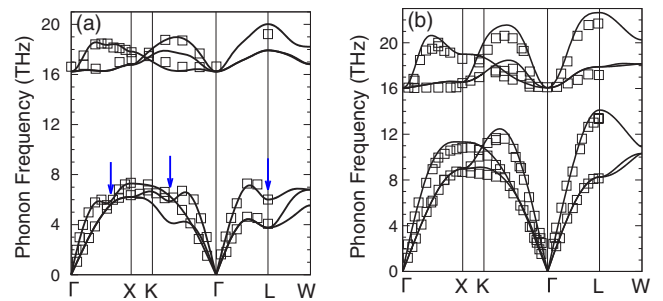


FIG. 2. Phonon dispersions of (a) NbC and (b) TiC calculated from first principles and compared to measured data from Refs. [42,43], respectively. Blue arrows in (a) show the phonon anomalies for NbC. No anomalies occur for TiC acoustic phonons.

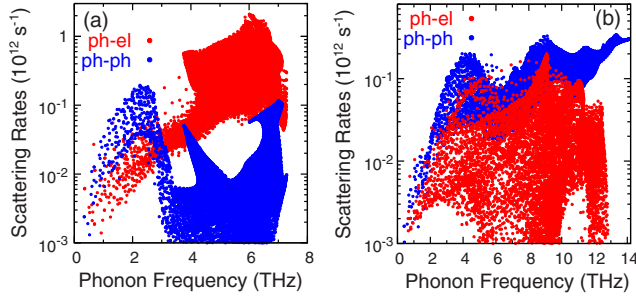


FIG. 3. Comparison of phonon-phonon (blue points) and phonon-electron (red points) scattering rates for (a) NbC and (b) TiC at 300 K.

Several features are responsible for the weak phonon-phonon scattering. To understand these, we first note that heat is carried primarily by the acoustic phonons. Intrinsic thermal resistance arises from scattering between three acoustic phonons (*aaa*), two acoustic phonons and an optic phonon (*aaopt*), or an acoustic phonon and two optic phonons (*aoopt*). The large mass of Nb atoms (92.91 amu) compared to C atoms (12.01 amu) produces a large frequency gap between acoustic and optic phonons, which forbids *aaopt* processes since they cannot satisfy energy conservation [44]. The narrow bandwidth of the optic phonon branches restricts *aoopt* processes to the region of low frequencies [45] where their scattering rates are weaker than *aaa* processes. Furthermore, Nb is isotopically pure. As a result, scattering of acoustic phonons by isotopic mass disorder is weak [13,46]. Thus, absent phonon-electron scattering,  $k_L$  is limited primarily by *aaa* scattering. Then, the bunched together regions of acoustic branches caused by these phonon anomalies severely restricts the phase space for *aaa* scattering, as has been pointed out previously [44]. These combined features give weak phonon-phonon and phonon-isotope scattering rates for the heat-carrying acoustic phonons. We note that higher-order four-phonon scattering has recently been found to be important in nonmetallic crystals with large frequency gaps between acoustic and optic phonons, such as BAs [47]. However, we expect that it would be much weaker than the phonon-electron scattering found here in NbC, VC, and TaC [16].

To highlight these contrasting behaviors, the phonon-phonon and phonon-electron scattering rates for NbC at 300 K are shown in Fig. 3(a) for the acoustic phonons. At low frequency, phonon-phonon scattering is stronger than phonon-electron scattering. With increasing frequency, a striking drop occurs in the phonon-phonon scattering rates (in the 4 to 8 THz regime), resulting from the small phase space for phonon-phonon scattering in this region. In the same frequency range, a large increase in the phonon-electron scattering rates is seen, driven by the FSN. Similar behavior of the Fermi surfaces, phonon dispersions, phonon-phonon and phonon-electron scattering rates is found for VC and TaC [16].

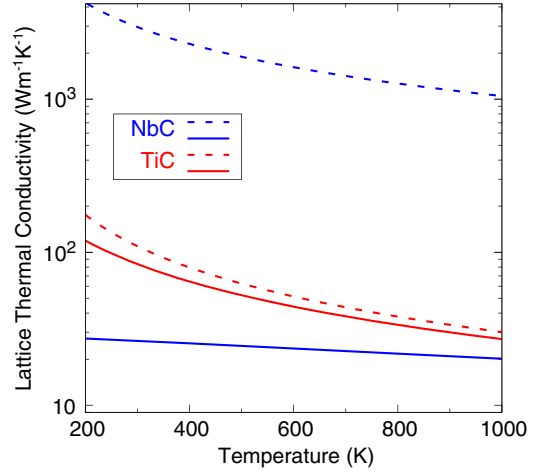


FIG. 4. Lattice thermal conductivity  $k_L$  as a function of  $T$  for NbC limited by (i) phonon-phonon and phonon-isotope scattering (dashed blue curve), (ii) phonon-phonon, phonon-isotope, and phonon-electron scattering (solid blue curve). Same for TiC with red curves.

The lattice thermal conductivity of NbC is shown in Fig. 4 for two cases: (i) limited by phonon-phonon and phonon-isotope scattering alone (dashed blue curve); (ii) including phonon-phonon, phonon-isotope, and phonon-electron scattering (solid blue curve). For case (i),  $k_L$  is extremely high, over  $3000 \text{ W m}^{-1} \text{ K}^{-1}$  at 300 K. These  $k_L$  values are comparable to or higher than the highest values achieved for a bulk crystal (i.e., diamond) over the same temperature range [48–50]. Including phonon-electron scattering, case (ii), decreases  $k_L$  by 2 orders of magnitude. This large reduction reflects the much stronger phonon-electron scattering compared to phonon-phonon scattering in the frequency region of the nesting vectors, as seen in Fig. 3(a). This results in a near temperature independence of  $k_L$  over the 300–1000 K range.

To contrast this unusual behavior for the group V TMCs, we have performed calculations for the group IV TMCs: TiC, ZrC, and HfC. Figures 1(b) and 2(b) show the Fermi surface and phonon dispersions for TiC. Some nesting appears to occur for small wave vectors [23] that may cause softening of the optic phonons around the  $\Gamma$  point. However, TiC shows no anomalies in the acoustic phonon spectrum. Figure 3(b) shows the phonon-phonon and phonon-electron scattering rates for TiC at 300 K. The phonon-phonon scattering rates for TiC are generally much larger than the phonon-electron scattering rates over the full acoustic phonon frequency range. As a result, for TiC the  $k_L$  neglecting phonon-electron scattering is seen to be almost the same as that including it, as shown in Fig. 4. The total  $k_L$  decreases roughly as  $1/T$  around and above 300 K, consistent with the temperature dependence of  $k_L$  in typical crystalline metals and nonmetals. Similar behavior is found for ZrC and HfC [16].

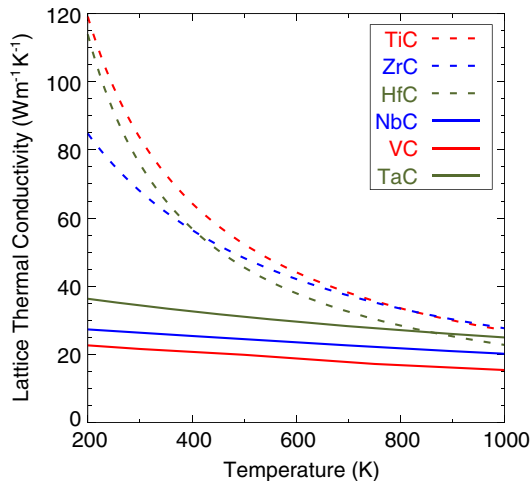


FIG. 5. Lattice thermal conductivity as a function of temperature for the group IV transition metal carbides, TiC, ZrC, and HfC (dashed curves), which show strong temperature dependence, and for the group V transition metal carbides, VC, NbC, and TaC, which show very little temperature dependence.

Figure 5 compares  $k_L$  for the six TMCs as a function of  $T$ . Consistent with the above discussion the  $k_L$  values decrease rapidly with  $T$  for all group IV TMCs, while those for the group V TMCs are almost temperature independent over the same  $T$  range. Around room temperature, group IV TMCs have far larger  $k_L$  than those of the group V TMCs, while at high  $T$  the  $k_L$  for the group IV TMCs are similar to those for the group V TMCs.

Experimental verification of the anomalous temperature dependence of  $k_L$  predicted here for the group V TMCs requires high quality samples. TMCs and TM nitrides typically have large concentrations of nonmetal (C and N) vacancies [9–12], which would strongly suppress the intrinsic  $k_L$  and make it temperature independent thereby masking the anomalous behavior. Recently, high quality growth of thin films of stoichiometric vanadium nitride (VN) has been achieved on MgO substrates [51]. The  $k_L$  extracted from measurements of the total thermal conductivity of VN [52] using the Wiedemann-Franz law and simple models for electronic structure and transport showed a relatively weak dependence on temperature in the 300–550 K range. As was pointed out in Ref. [52], VN should have strong electron-phonon scattering given its rather high superconducting transition temperature  $\sim 9$  K [9]. Since our computational approach does not determine temperature dependent IFCs, we are not able to capture the phonon behavior of VN in the rock salt phase and so cannot directly calculate  $k_L$  to compare to the measured data. Instead, we have calculated the Fermi surface of VN in the rocksalt structure [16], which indeed shows nested regions whose nesting vector corresponds to the phonon anomaly around the  $X$  point observed in the measured phonon dispersions [52]. However, the frequency gap between acoustic and optic phonons [53] is not large enough to freeze out  $aa_0$

scattering processes. This suggests that phonon-phonon scattering is not weak in VN. In fact, extrapolating the roughly linear  $k_L$  found in Ref. [52] to higher  $T$  predicts a factor of 2 reduction in  $k_L$  at 1000 K compared to that at 300 K, far larger than the corresponding reductions in the calculated  $k_L$  values of VC, NbC, and TaC.

The electronic and phonon properties responsible for the anomalously weak  $T$  dependence of  $k_L$  found here in the group V TMCs occur in other compounds. Specifically, ZrN and HfN both show FSN and phonon anomalies [24,54] and their electron-phonon coupling constants are large [24]. Also, their phonon dispersions show large frequency gaps between acoustic and optic phonons. As a result, we speculate that near  $T$  independent  $k_L$  should also occur in these compounds over a similarly large  $T$  range around and above room temperature. TiN, ScC, and YC also exhibit nesting [24,55] and have larger electron-phonon coupling constants [24] suggesting that electron-phonon scattering should be strong. However, their frequency gaps between acoustic and optic phonons are not sufficiently large to freeze-out the scattering between the heat-carrying acoustic phonons and optic phonons. Therefore, we predict a stronger  $T$  dependence of  $k_L$  in these compounds above 300 K than should occur in VC, NbC, TaC, ZrN, or HfN, but still weaker than the typical phonon-phonon scattering dominated behavior, qualitatively similar to that found in VN [52]. We note that large suppression of  $k_L$  was recently predicted for highly doped Si where phonon-electron and phonon-phonon scattering rates were found to be similar for carrier densities around  $10^{21}$  cm $^{-3}$  [56], though doped Si does not have a nested Fermi surface and the suppression was much smaller than found here for the group V TMCs.

To summarize, employing first principles calculations, we demonstrate that in metals with nested Fermi surfaces and large frequency gaps between heat-carrying acoustic phonons and optic phonons an unusual combination of weak phonon-phonon interactions and strong electron-phonon interactions occurs. This combination, the reverse of the typical behavior in both metallic and non-metallic crystals, is predicted for several transition metal carbide (VC, NbC, and TaC) and nitride (ZrN and HfN) compounds. It gives a nearly temperature independent lattice thermal conductivity to well above room temperature in striking contrast to the rapid decrease of lattice thermal conductivity with temperature normally found in crystalline solids. This work gives new insights into heat conduction in solids and identifies an anomalous regime of transport behavior whose experimental verification should be possible through growth and characterization of high-quality crystals of the identified metal compounds.

C. L. and D. B. acknowledge support from the National Science Foundation under Grant No. 1402949. C. L., N. K. R. and D. B. acknowledge support from the Office of Naval Research Multidisciplinary University Research

Initiative, Grant No. N00014-16-1-2436. L. L. acknowledges support from the U.S. Department of Energy, Office of Science, Office of Basic Energy Sciences, Materials Sciences and Engineering Division for work done at ORNL. The computational part of this research used resources of the Extreme Science and Engineering Discovery Environment (XSEDE), which is supported by National Science Foundation Grant No. TG-ASC160070 and No. ACI-1548562, and the Boston College linux clusters.

\*Corresponding author.  
broido@bc.edu

- [1] R. E. Peierls, *Quantum Theory of Solids* (Clarendon Press, Oxford 1955).
- [2] J. M. Ziman, *Electrons and Phonons* (Oxford University Press, London, 1960).
- [3] R. E. B. Makinson, The thermal conductivity of metals, *Math. Proc. Cambridge Philos. Soc.* **34**, 474 (1938).
- [4] A. Jain and A. J. H. McGaughey, Thermal transport by phonons, and electrons in aluminum, silver, and gold from first principles, *Phys. Rev. B* **93**, 081206(R) (2016).
- [5] Y. Wang, Z. Lu, and X. Ruan, First principles calculation of lattice thermal conductivity of metals considering phonon-phonon, and phonon-electron scattering, *J. Appl. Phys.* **119**, 225109 (2016).
- [6] P. A. Lee, N. Nagaosa, and X.-G. Wen, Doping a Mott insulator: Physics of high-temperature superconductivity, *Rev. Mod. Phys.* **78**, 17 (2006).
- [7] M.-H. Whangbo, E. Canadell, P. Foury, and J.-P. Pouget, Hidden Fermi surface nesting and charge density wave instability in low-dimensional metals, *Science* **252**, 96 (1991).
- [8] F. Giustino, Electron-phonon interactions from first principles, *Rev. Mod. Phys.* **89**, 015003 (2017).
- [9] L. E. Toth, *Refractory Materials A Series of Monographs, Volume 7: Transition Metal Carbides and Nitrides* (Academic Press, New York, 1971).
- [10] H. O. Pierson, *Handbook of Refractory Carbides and Nitrides* (Noyes Publications, New Jersey, 1996).
- [11] Y. Kumashiro, *Electric Refractory Materials* (Marcel Dekker, Inc, New York, 2000).
- [12] V. A. Gubanov, A. L. Ivanovsky, and V. P. Zhukov, *Electronic Structure of Refractory Carbides and Nitrides* (Cambridge University Press, 2005).
- [13] S.-i. Tamura, Isotope scattering of large wave-vector phonons of GaAs, and InSb: Deformation-dipole, and overlap shell models, *Phys. Rev. B* **30**, 849 (1984).
- [14] S. Baroni, S. Gironcoli, A. D. Corso, and P. Giannozzi, Phonons and related crystal properties from density-functional perturbation theory, *Rev. Mod. Phys.* **73**, 515 (2001).
- [15] K. Esfarjani and H. T. Stokes, Method to extract anharmonic force constants from first principles calculations, *Phys. Rev. B* **77**, 144112 (2008).
- [16] See Supplementary Materials at <http://link.aps.org/supplemental/10.1103/PhysRevLett.121.175901>, for computational details of phonon dispersions, three-phonon, phonon-electron and phonon-isotope scattering rates, corroboration of nesting vectors with location of phonon anomalies, consideration of four-phonon scattering, plots of Fermi surfaces, phonon dispersions and three-phonon scattering rates for VC, TaC, ZrC, and HfC, and Fermi surface of VN, which includes Refs. [17–22].
- [17] J. P. Perdew, K. Burke, and M. Ernzerhof, Generalized Gradient Approximation Made Simple, *Phys. Rev. Lett.* **77**, 3865 (1996).
- [18] K. Nakamura and M. Yashima, Crystal structure of NaCl-type transition metal monocarbides MC (M = V, Ti, Nb, Ta, Hf, Zr), a neutron powder diffraction study, *Mater. Sci. Eng. B* **148**, 69 (2008).
- [19] A. A. Maradudin, E. W. Montroll, and G. H. Weiss, Theory of lattice dynamics in the harmonic approximation, in *Solid State Physics* (Academic Press, New York, 1963), Supplement 3.
- [20] W. Li, L. Lindsay, D. Broido, D. A. Stewart, and N. Mingo, Thermal conductivity of bulk, and nanowire  $\text{Mg}_2\text{Si}_x\text{Sn}_{1-x}$  alloys from first principles, *Phys. Rev. B* **86**, 174307 (2012).
- [21] J. Shiomi, K. Esfarjani, and G. Chen, Thermal conductivity of half-Heusler compounds from first-principles calculations, *Phys. Rev. B* **84**, 104302 (2011).
- [22] D. Zaharioudakis, Tetrahedron methods for Brillouin zone integration, *Comput. Phys. Commun.* **157**, 17 (2004).
- [23] J. Noffsinger, F. Giustino, S. G. Louie, and M. L. Cohen, First-principles study of superconductivity, and Fermi-surface nesting in ultrahard transition metal carbides, *Phys. Rev. B* **77**, 180507(R) (2008).
- [24] E. I. Isaev, S. I. Simak, I. A. Abrikosov, R. Ahuja, Yu. Kh. Vekilov, M. I. Katsnelson, A. I. Lichtenstein, and B. Johansson, Phonon related properties of transition metals, their carbides, and nitrides: A first principles study, *J. Appl. Phys.* **101**, 123519 (2007).
- [25] F. Giustino, M. L. Cohen, and S. G. Louie, Electron-phonon interaction using Wannier functions, *Phys. Rev. B* **76**, 165108 (2007).
- [26] J. Noffsinger, F. Giustino, B. D. Malone, C.-H. Park, S. G. Louie, and M. L. Cohen, EPW: A program for calculating the electron-phonon coupling using maximally localized Wannier functions, *Comput. Phys. Commun.* **181**, 2140 (2010).
- [27] S. Poncé, E. R. Margine, C. Verdi, and F. Giustino, EPW: Electron-phonon coupling, transport and superconducting properties using maximally localized Wannier functions, *Comput. Phys. Commun.* **209**, 116 (2016).
- [28] H. Smith and H. Jensen, *Transport Phenomena* (Clarendon Press, Oxford 1989).
- [29] P. Giannozzi *et al.*, QUANTUM ESPRESSO: a modular and open-source software project for quantum simulations of materials, *J. Phys. Condens. Matter* **21**, 395502 (2009).
- [30] P. Giannozzi *et al.*, Advanced capabilities for materials modelling with Quantum ESPRESSO, *J. Phys. Condens. Matter* **29**, 465901 (2017).
- [31] <http://epw.org.uk/Main/HomePage>.
- [32] M. Omini, A. Sparavigna, An iterative approach to the phonon Boltzmann equation in the theory of thermal conductivity, *Physica (Amsterdam)* **212B**, 101 (1995).

- [33] D. A. Broido, A. Ward, and N. Mingo, Lattice thermal conductivity of silicon from empirical interatomic potentials, *Phys. Rev. B* **72**, 014308 (2005).
- [34] D. A. Broido, M. Malorny, G. Birner, N. Mingo, and D. A. Stewart, Intrinsic lattice thermal conductivity of semiconductors from first principles, *Appl. Phys. Lett.* **91**, 231922 (2007).
- [35] W. Li, J. Carrete, N. Katcho, and N. Mingo, ShengBTE: A solver of the Boltzmann transport equation for phonons, *Comput. Phys. Commun.* **185**, 1747 (2014).
- [36] W. Weber, Lattice dynamics of transition-metal carbides, *Phys. Rev. B* **8**, 5082 (1973).
- [37] B. M. Klein, L. L. Boyer, and D. A. Papaconstantopoulos, On the relationship between the phonon anomalies and the *ab initio* calculated Fermi surfaces of TaC and NbC, *Solid State Commun.* **20**, 937 (1976).
- [38] A. Nørnlund Christensen, W. Kress, M. Miura, and N. Lehner, Phonon anomalies in transition-metal nitrides: HfN, *Phys. Rev. B* **28**, 977 (1983).
- [39] H. G. Smith, Phonon Anomalies in Transition-Metal Carbides, *Phys. Rev. Lett.* **29**, 353 (1972).
- [40] Correspondence between the locations of the phonon anomalies and the nesting vectors is shown in Ref. [16].
- [41] A. Kokalj, XCrySDen—a new program for displaying crystalline structures and electron densities, *J. Mol. Graphics Modell.* **17**, 176 (1999).
- [42] H. G. Smith and W. Gläzer, Phonon spectra and superconductivity in some transition metal carbides, in *Proceedings of the International Conference on Phonons, Rennes, France*, edited by M. A. Nusimovici (Flammaron Sciences, Paris, 1971).
- [43] L. Pintschovius, W. Reichardt, and B. Scheerer, Lattice dynamics of TiC, *J. Phys. C* **11**, 1557 (1978).
- [44] L. Lindsay, D. A. Broido, and T. L. Reinecke, First-Principles Determination of Ultrahigh Thermal Conductivity of Boron Arsenide: A Competitor for Diamond?, *Phys. Rev. Lett.* **111**, 025901 (2013).
- [45] S. Mukhopadhyay, L. Lindsay, and D. S. Parker, Optic phonon bandwidth and lattice thermal conductivity: The case of  $\text{Li}_2\text{X}$  ( $\text{X} = \text{O}, \text{S}, \text{Se}, \text{Te}$ ), *Phys. Rev. B* **93**, 224301 (2016).
- [46] M. Lax, P. Hu, and V. Narayanamurti, Spontaneous phonon decay selection rule: N and U processes, *Phys. Rev. B* **23**, 3095 (1981).
- [47] T. Feng, L. Lindsay, and X. Ruan, Four-phonon scattering significantly reduces intrinsic thermal conductivity of solids, *Phys. Rev. B* **96**, 161201(R) (2017).
- [48] D. G. Onn, A. Witek, Y. Z. Qiu, T. R. Anthony, and W. F. Banholzer, Some Aspects of the Thermal Conductivity of Isotopically Enriched Diamond Single Crystal, *Phys. Rev. Lett.* **68**, 2806 (1992).
- [49] L. Wei, P. K. Kuo, R. L. Thomas, T. R. Anthony, and W. F. Banholzer, Thermal Conductivity of Isotopically Modified Single Crystal Diamond, *Phys. Rev. Lett.* **70**, 3764 (1993).
- [50] J. R. Olson, R. O. Pohl, J. W. Vandersande, A. Zoltan, T. R. Anthony, and W. F. Banholzer, Thermal conductivity of diamond between 170 and 1200 K and the isotope effect, *Phys. Rev. B* **47**, 14850 (1993).
- [51] A. B. Mei, O. Hellman, N. Wireklint, C. M. Schlepütz, D. G. Sangiovanni, B. Alling, A. Rockett, L. Hultman, I. Petrov, and J. E. Greene, Dynamic and structural stability of cubic vanadium nitride, *Phys. Rev. B* **91**, 054101 (2015).
- [52] Q. Zheng, A. B. Mei, M. Tuteja, D. G. Sangiovanni, L. Hultman, I. Petrov, J. E. Greene, and D. G. Cahill, Phonon, and electron contributions to the thermal conductivity of VN<sub>x</sub> epitaxial layers, *Phys. Rev. Mater.* **1**, 065002 (2017).
- [53] W. Weber, P. Roedhammer, L. Pintschovius, W. Reichardt, F. Gompf, and A. N. Christensen, Phonon Anomalies in VN and Their Electronic Origin, *Phys. Rev. Lett.* **43**, 868 (1979).
- [54] A. N. Christensen, O. W. Dietrich, W. Kress, and W. D. Teuchert, Phonon anomalies in transition-metal nitrides: ZrN, *Phys. Rev. B* **19**, 5699 (1979).
- [55] W. Kress, P. Roedhammer, H. Bilz, W. D. Teuchert, and A. N. Christensen, Phonon anomalies in transition-metal nitrides: TiN, *Phys. Rev. B* **17**, 111 (1978).
- [56] B. Liao, B. Qiu, J. Zhou, S. Huberman, K. Esfarjani, and G. Chen, Significant Reduction of Lattice Thermal Conductivity by the Electron-Phonon Interaction in Silicon with High Carrier Concentrations: A First-Principles Study, *Phys. Rev. Lett.* **114**, 115901 (2015).